Pharmacological Research 178 (2022) 106149

Contents lists available at ScienceDirect

Pharmacological Research

journal homepage: www.elsevier.com/locate/yphrs

Therapeutic induction of energy metabolism reduces neural tissue damage and increases microglia activation in severe spinal cord injury

Sissi Dolci [a,1], Loris Mannino [a,1], Emanuela Bottani [a,1], Alessandra Campanelli [a], Marzia Di Chio [a], Stefania Zorzin [a], Giulia D'Arrigo [b], Alessia Amenta [c], Agnese Segala [d], Giuseppe Paglia [e], Vanna Denti [e], Guido Fumagalli [a], Enzo Nisoli [f], Alessandra Valerio [d], Claudia Verderio [b], Giuseppe Martano [b], Francesco Bifari [c,*], Ilaria Decimo [a,**]

[a] Department of Diagnostic and Public Health, Section of Pharmacology, University of Verona, 37134, Italy
[b] CNR Institute of Neuroscience, Milan 20854, Italy
[c] Laboratory of Cell Metabolism and Regenerative Medicine, Department of Medical Biotechnology and Translational Medicine, University of Milan, 20133, Italy
[d] Department of Molecular and Translational Medicine, University of Brescia, 25121, Italy
[e] School of Medicine and Surgery, University of Milano-Bicocca, 20126, Italy
[f] Center for Study and Research on Obesity, Department of Medical Biotechnology and Translational Medicine, University of Milan, 20133, Italy

ARTICLE INFO

Keywords:
Spinal cord injury
Cell metabolism
Mitochondrial metabolism
Neural regeneration
Microglia

ABSTRACT

Neural tissue has high metabolic requirements. Following spinal cord injury (SCI), the damaged tissue suffers from a severe metabolic impairment, which aggravates axonal degeneration and neuronal loss. Impaired cellular energetic, tricarboxylic acid (TCA) cycle and oxidative phosphorylation metabolism in neuronal cells has been demonstrated to be a major cause of neural tissue death and regeneration failure following SCI. Therefore, rewiring the spinal cord cell metabolism may be an innovative therapeutic strategy for the treatment of SCI. In this study, we evaluated the therapeutic effect of the recovery of oxidative metabolism in a mouse model of severe contusive SCI. Oral administration of TCA cycle intermediates, co-factors, essential amino acids, and branched-chain amino acids was started 3 days post-injury and continued until the end of the experimental procedures. Metabolomic, immunohistological, and biochemical analyses were performed on the injured spinal cord sections. Administration of metabolic precursors enhanced spinal cord oxidative metabolism. In line with this metabolic shift, we observed the activation of the mTORC1 anabolic pathway, the increase in mitochondrial mass, and ROS defense which effectively prevented the injury-induced neural cell apoptosis in treated animals. Consistently, we found more choline acetyltransferase (ChAT)-expressing motor neurons and increased neurofilament-positive corticospinal axons in the spinal cord parenchyma of the treated mice. Interestingly, oral administration of the metabolic precursors increased the number of activated microglia expressing the CD206 marker suggestive of a pro-resolutive, M2-like phenotype. These molecular and histological modifications observed in treated animals ultimately led to a significant, although partial, improvement of the motor functions. Our data demonstrate that rewiring the cellular metabolism can represent an effective strategy to treat SCI.

1. Introduction

To accomplish its multiple and energetic demanding functions, the neural tissue has a high metabolic rate (3.5 ml O_2/100 g/min corresponding to approximately 4×10^{21} molecules of ATP/min) [1], required to ensure axonal elongation, dendrite morphogenesis, generation of the action potential, synaptic transmission, maturation, and plasticity [2–4]. Following spinal cord injury (SCI), neural cells

Abbreviations: SCI, spinal cord injury; OXPHOS, oxidative phosphorylation; TCA, tricarboxylic acid; EAAs, essential amino acids; BCAAs, branched-chain amino acids.

* Correspondence to: Department of Medical Biotechnology and Translational Medicine, University of Milan, Via Vanvitelli, 32, 20129 Milan, Italy.
** Correspondence to: Department of Diagnostics and Public Health, Section of Pharmacology, University of Verona, P.le Scuro 10, 37134 Verona, Italy.
E-mail addresses: francesco.bifari@unimi.it (F. Bifari), ilaria.decimo@univr.it (I. Decimo).

[1] These authors contributed equally to this work and share co-first authorship

https://doi.org/10.1016/j.phrs.2022.106149
Received 4 January 2022; Received in revised form 16 February 2022; Accepted 26 February 2022
Available online 28 February 2022

experience a dramatic metabolic impairment with more than 25% of the metabolome significantly altered [5]. Metabolic alterations contribute to the loss of crucial cellular functions such as ion/anion pumping (*i.e.* Na/K or H_2CO_3), and the mitochondrial membrane potential [6]. These events lead to the impairment of the tricarboxylic acid (TCA) cycle and oxidative phosphorylation (OXPHOS) [7,8] that worsen the disease progression and promote glutamate excitotoxicity-driven-neuronal cell death [9].

The modulation of cellular metabolism is nowadays considered an attractive and innovative strategy for restoring neural cell functions [10]. In the developing cortex, the increase of OXPHOS metabolism *via* inhibition of the glycolytic enzyme PFKFB3 drives neuronal differentiation [11]. Enhancement of the oxidative pentose phosphate pathway (oxPPP) improves neural tissue survival following acute cerebral ischemia [12]. Moreover, the restoration of energy metabolism through anaplerosis counteracts the severe OXPHOS deficiency, and thereby confers metabolic resilience to Purkinje neuronal death in a mouse model of motor-sensory neuropathy [13]. The antioxidant molecules N-acetyl-cysteine (NAC) and acetyl-L-carnitine (ALC) attenuate retrograde neuronal degeneration after peripheral nerve injury and following SCI [14]. Systemic administration of ALC to SCI mice increases mitochondrial function and tissue sparing, both rostral and caudal of the injury site [8].

We have shown that the administration of essential amino acids (EAAs) enriched in branched-chain amino acids (BCAAs) and metabolic substrates increases TCA, OXPHOS, and the mammalian/mechanistic Target of Rapamycin Complex 1 (mTORC1)-driven energy metabolism in neuronal cells *in vitro* [15]. Such energetic availability enhances neuronal axonal branching, synaptic maturation, and NRF2-mediated antioxidant defense [15]. Recently, a proof-of-concept study provided evidence that energetic impairment in neuronal cells is responsible for neural tissue death and regeneration failure following SCI [16]. A transgenic animal model with enhanced mitochondrial transport improves cortico-spinal tract axonal regeneration following SCI [16]. Moreover, administration of the bioenergetic compound creatinine in dorsal hemisected spinal cord animals increases some axonal sprouting through the lesion site, and this effect is greatly amplified in combination with increased mitochondrial transport [16].

These data strongly suggest that enhancing the energetic metabolism of spinal cord cells could boost the regenerative capacity following severe contusive SCI. However, whether a therapeutic modulation of the neural tissue metabolism following SCI can counteract the neural tissue loss and improve neuronal regeneration is still not known.

In this work, we showed that therapeutic (from 3 day-post injury) oral administration of metabolic substrates i) induced TCA and OXPHOS metabolism in spinal cord tissue, ii) improved the mTORC1-related anabolic pathway in neurons, iii) increased mitochondrial mass and respiration, and iv) reduced oxidative stress at the site of the lesion. In addition, treated animals increased the intraspinal microglial population, which appeared more activated. Consistently, treated SCI animals showed increased axonal content through the lesion, neuronal cell number, and partial motor recovery.

2. Materials and methods

2.1. Severe contusive SCI-mouse model

All experimental procedures were approved by Istituto Superiore di Sanità (I.S.S., National Institute of Health; protocol N.154/2014-B, Italy) and the Animal Ethics Committee (C.I.R.S.A.L., Centro Interdipartimentale di Servizio alla Ricerca Sperimentale) of the University of Verona (Italy). Severe contusive spinal cord injury was performed as described [17]. Briefly, seven-week-old C57BL/6 female mice were anesthetized with 2% isoflurane, and laminectomy was performed at T11 level. A 5-gr rod was dropped from 6,25 mm height using a MASCIS Impactor and left in compression for 11 s

2.2. α5 administration

The administration of α5 was performed in drinking water (dose 3 mg/g/day), starting at 3 days post-injury (DPI) as shown in Fig. 1B.

2.3. Locomotor evaluation

Locomotor activity was blindly evaluated according to the Basso Mouse Scale (BMS) [18]. Mice with a BMS score ≤ 0.5 at 1 DPI were randomly assigned to the vehicle- or α5-treated groups.

2.4. Flexibility of the ankle joint

The analysis was performed from 21 DPI to evaluate the spasticity of the muscles involved in the ankle dorsiflexors and plantarflexors [19]; the following scores were assigned: "0" to the lack of movement (spastic condition, corresponding to an angle of 180° between the *tibialis anterior* and the paw), "0.25" to an angle of 135°, "0.5" to an angle of 90°, "0.75" to an angle of 45°, and "1" to a normal movement corresponding to an angle of 0 ° (Fig. 4I).

2.5. Targeted metabolomics

Analysis of the lesioned spinal tract (0.5 cm of dissected spinal cords, 0.25 cm rostral, and 0.25 cm caudal from the site of the lesion) was performed at 14 DPI as described [20–22]. Detailed descriptions of the methods are in the supplementary information.

2.6. Spinal cord fixation and processing

Animals were intracardially perfused with 4% paraformaldehyde (PFA) and 4% sucrose. Spinal cords were extracted, immersed overnight in 4% PFA, 4% sucrose, and stored in 30% sucrose at 4 °C. For histochemical analysis, 1.5 cm of dissected spinal cords (0.75 cm rostral and 0.75 cm caudal from the site of the lesion) were cryosectioned (25 μm-thick transverse sections or 20 μm-thick longitudinal sections) and stored at − 20 °C before analysis.

2.7. Luxol fast blue staining

Myelin content was quantified in the spinal cord sections *via* Luxol Fast Blue (LFB) staining (Sigma-Aldrich) as described [23].

2.8. Immunofluorescence

Cryosections were blocked in 0.25% or 0.5% Triton X-100, 2% BSA, and incubated with primary and secondary antibodies (listed in supplementary information). Nuclei were stained with TO-PRO™-3 (Thermo Fisher Scientific) or 4'.6-Diamidino-2-Phenylindole (DAPI, Thermo Fisher Scientific, 1:2000) and slices were mounted using 1.4-Diazabicyclo (2.2.2) octane (DABCO, Sigma Aldrich). Images were acquired using a 63x oil objective (Carl Zeiss LSM710 confocal microscope, Munich, Germany), and a 20x objective (Nikon Ti Eclipse fluorescent microscope).

2.9. Immunoblot analysis

Either microglial cells or spinal cord sections (0.5 cm of dissected spinal cords, of which 0.25 cm rostral and 0.25 cm caudal from the site of the lesion) were homogenized in RIPA buffer as described [24]; 20 μg of proteins were run through a 4–12% SDS–polyacrylamide gel electrophoresis, electroblotted onto a PVDF membrane, and probed with different primary antibodies listed in the supplementary information file. Chemiluminescence-based immunostainings were acquired with the ImageQuant LAS 4000 apparatus (GE Healthcare) and/or Chemidoc MP Imaging System (Bio-Rad); and quantified with Image Lab™

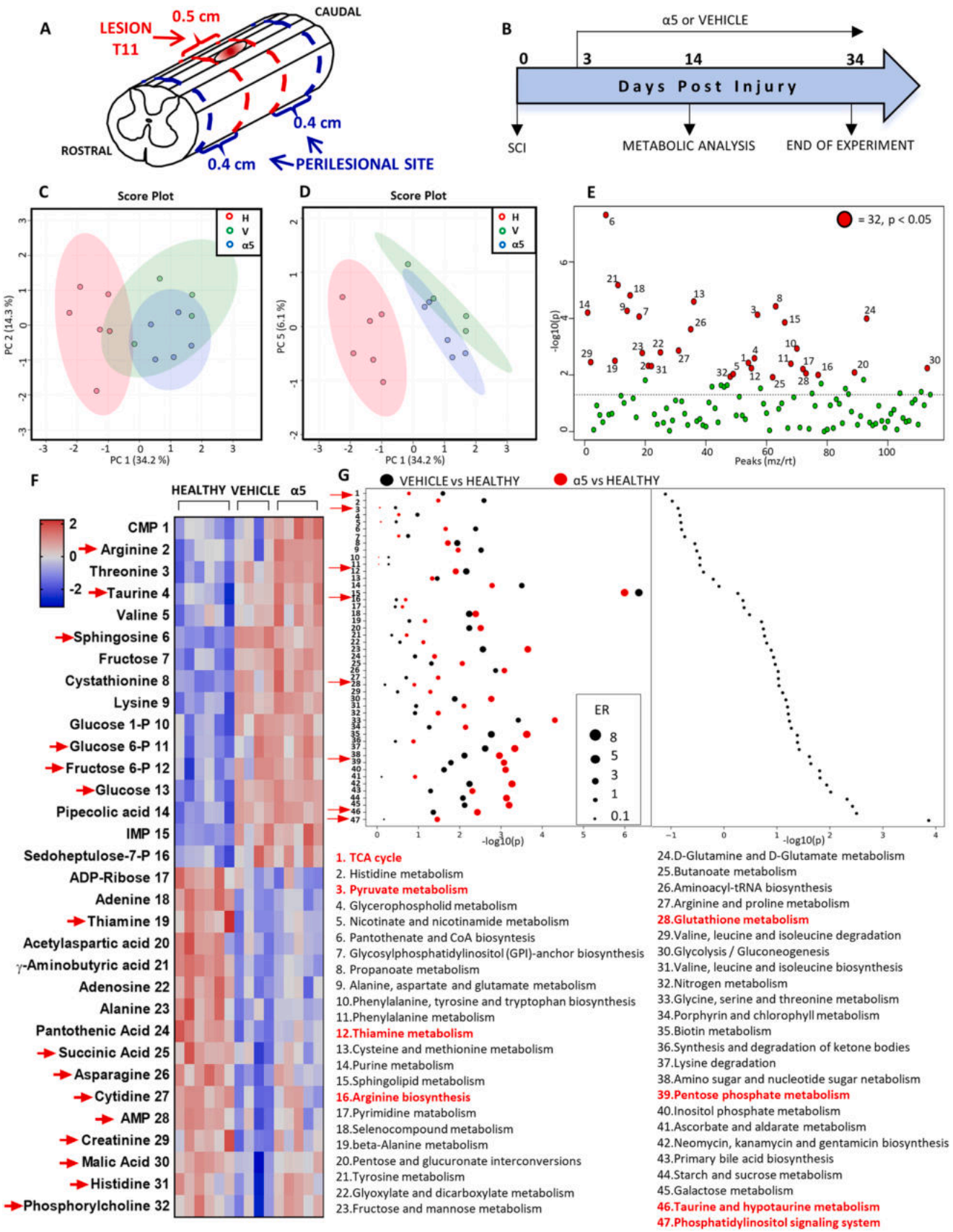

(caption on next page)

Fig. 1. Functional metabolic rewiring of the injured spinal cord upon α5 supplementation. A) Schematic drawing of the spinal cord highlighting the site of the lesion (T11 vertebra), the 0.5 cm injured fragment (red dashed lines) analyzed by LC-MS, and the perilesional area (blue dashed lines) evaluated for morpho-functional studies; the spinal cord section corresponding to the 0.5 cm lesion site was also analyzed in the unlesioned, vehicle-treated healthy mice by LC-MS for comparison. B) Timeline of the experimental setting. C) and D) Principal component analysis (PCA) of the metabolites analyzed in the vehicle-treated (green ellipse), α5-treated (blue ellipse), and healthy (red ellipse) spinal cord tissues. E) Schematic representation of the results of the 1-way ANOVA analysis (expressed as log10 (p-value)) of the metabolites detected by LC-MS (indicated as peak mz/rt). Red dots represent the 32 metabolites - listed in F - significantly modulated in the three experimental groups. F) Heatmap showing the mean values – as z-score - of the metabolites differentially regulated within the 3 groups. G) Pathway enrichment analysis built by comparing the lesioned α5-treated (red dots) and vehicle-treated (black dots) mice against the healthy group. Enrichment ratio (ER) is shown as dot size and ΔER represents the difference between the ER from lesioned α5-treated and the ER from vehicle-treated mice. Data are collected at 14 DPI, N = 6 healthy, 4 vehicle- and 5 α5-treated mice/group. DPI = day post-injury. Data are expressed as mean ± SEM, statistical analysis was performed with 1-way ANOVA and Tukey *post hoc* test for comparison, * $p < 0.05$, * * $p < 0.01$.

software, version 6.0.1 (Bio-Rad).

2.10. Mitochondrial DNA quantification

Total DNA was quantified with the Qubit dsDNA HS Assay Kit and Qubit 4 fluorometer (Invitrogen, Life Technologies). The Droplet digital PCR was performed using the QX200 Droplet Digital PCR System (Bio-Rad). Primers targeting the MT-ND1 gene were used to amplify the mtDNA (primes sequences as in [25]).

2.11. Extracellular flux analysis of isolated spinal cord mitochondria

Mitochondrial fractions were obtained from 0.5 cm thick spinal cord sections (0.25 cm rostral and 0.25 cm caudal from the site of the lesion) as described [26]. Assays were performed on 7 μg of mitochondria by measuring the oxygen consumption rate (OCR) in Mitochondrial Assay Solution (MAS1) with complex I (10 mM Glutamate and 5 mM Malate) and complex II (10 mM Succinate) substrates at the basal level and after subsequent injection of 4 mM ADP, 3.1 μM oligomycin, 4 μM FCCP and 2 μM Rotenone plus 4 μM Antimycin A. Data were analyzed as reported [26].

2.12. Image analyses and quantification

The quantitative analysis was done with NIH ImageJ software [U.S. National Institutes of Health]. Ten to forty transversal sections and five to twenty-seven longitudinal sections of the spinal cord were analyzed in at least 2–4 technical replicates (glass slides). For the analysis normalized to the number of total nuclei, approximately 5115 ± 87 nuclei were considered. Three to five mice were considered for the analysis; the exact number of mice is reported in each graph.

2.13. Statistical analysis

GraphPad Prism software (version 7.0) was used to perform unpaired two-sided Student's t-test, one-way ANOVA repeated measures followed by Tukey post-test, two-way ANOVA with repeated measures. Data are shown as mean ± SEM and statistical significance was set at $p < 0.05$.

Other detailed methods are reported in Supplementary Material.

3. Results

3.1. Therapeutic administration of α5 promotes metabolic recovery in the damaged spinal cord after severe SCI

SCI induced a profound metabolic impairment to the neural tissue [5]. To rescue the neural cell metabolism following SCI, we administered a selection of bioenergetic molecules (Table 1), including the TCA cycle intermediates, essential amino acids (EAAs), branched-chain amino acids (BCAAs), and the cofactors thiamine and pyridoxine - altogether referred to as α5 - known to improve the OXPHOS metabolism in neuronal cells *in vitro* [15] and mitochondrial activity in muscle and brain *in vivo* [24,27]. BCAAs and EAAs act as substrates that can replenish TCA cycle intermediates through anaplerotic reactions; moreover, BCAAs, mainly leucine, boost the anabolic function of the mTORC1 [28–30] and positively regulate mitochondrial oxidative function [31,32]. Thiamine is essential for normal brain function [33].

First, to exclude that α5 may impair basal metabolism, we confirmed that chronic administration of α5 in C57BL/6 healthy mice did not affect neither the body weight (Suppl. Fig. S1A) nor the cage activity (Suppl. Fig. S1G-J), despite a slight modulation of the food and water intake (Suppl. Fig. S1B-D), that did not affect the daily caloric intake (Suppl. Fig. S1E-F). Then, to assess the therapeutic effects of a chronic, oral α5 administration, severe spinal cord injured C57BL/6 mice (See Fig. 1A and Section 2.1 for the description of the SCI model) were treated daily from day 3 post-injury (DPI) with either α5 or vehicle (Fig. 1B).

At 14 DPI, we evaluated whether α5 treatment produced a metabolic modulation of the injured spinal cord through targeted metabolomic analysis. A drastic impairment of the metabolome of the lesioned spinal cord was confirmed, being 38 out of 114 (corresponding to 40.3%, healthy *vs* vehicle SCI group, unpaired t-test, $p < 0.05$) of the analyzed metabolite altered compared to the healthy, uninjured, and vehicle-treated spinal cord. Differences among healthy, α5- or vehicle-treated groups were also compared with principal component analysis (PCA) using the metabolic fingerprint of each sample (Fig. 1 C, D). As expected, major differences between SCI groups were found in comparison with the healthy group (Fig. 1 C). However, differences introduced by the treatment, represented by the 5th component, accounted for 6.1% of the variance (Fig. 1D). Differentially regulated metabolites assessed by ANOVA comparison among healthy, α5- or vehicle-treated groups, identified 32 differentially regulated metabolites (Fig. 1E). Major dysregulations introduced by SCI were found in metabolites involved in the TCA cycle (Fig. 1 F, G). The α5 treatment rescued the levels of TCA cycle intermediates malate and succinate, that were impaired in the vehicle group, close to the levels found in healthy mice (Fig. 1 F). This suggests an increase in oxidative metabolism (see Section 3.2). The glycolytic intermediates (glucose, fructose 6-phosphate, glucose 6-phosphate) were significantly higher in the vehicle-treated group, possibly as a compensatory mechanism consequent to mitochondrial impairment [8,34] (Fig. 1 F). High levels of glycolytic intermediates persisted also in α5-treated SCI mice, suggesting that energy metabolism, in this condition, could use both glycolysis and TCA cycle (Fig. 1 F).

We then performed a pathway enrichment analysis by comparing the lesioned α5-treated and vehicle-treated tissues against the healthy group (Fig. 1 G). To elucidate the impact of the treatment, we calculated the ΔER, which represents the difference between the enrichment ratios of the two enrichment sets, confirming that the most significant differences were found in the TCA cycle (Fig. 1G). Moreover, we observed differences in several metabolic processes including the phosphatidylinositol signaling pathway, taurine, and hypotaurine metabolism, thiamine metabolism, glutathione and oxPPP, and arginine biosynthesis. The phosphatidylinositol signaling pathway was highly enriched in the α5-treated group (Fig. 1G). Phosphoinositides (PIs) act as signaling molecules in the PI3K/Akt/mTOR cascade, which has a central role in cellular metabolism, cell growth, cytoskeletal changes, and actin remodeling [35]. Taurine metabolism was activated in the vehicle-treated injured spinal cords and further increased in the α5-treated mice (Fig. 1F, G). Taurine is synthesized from methionine and

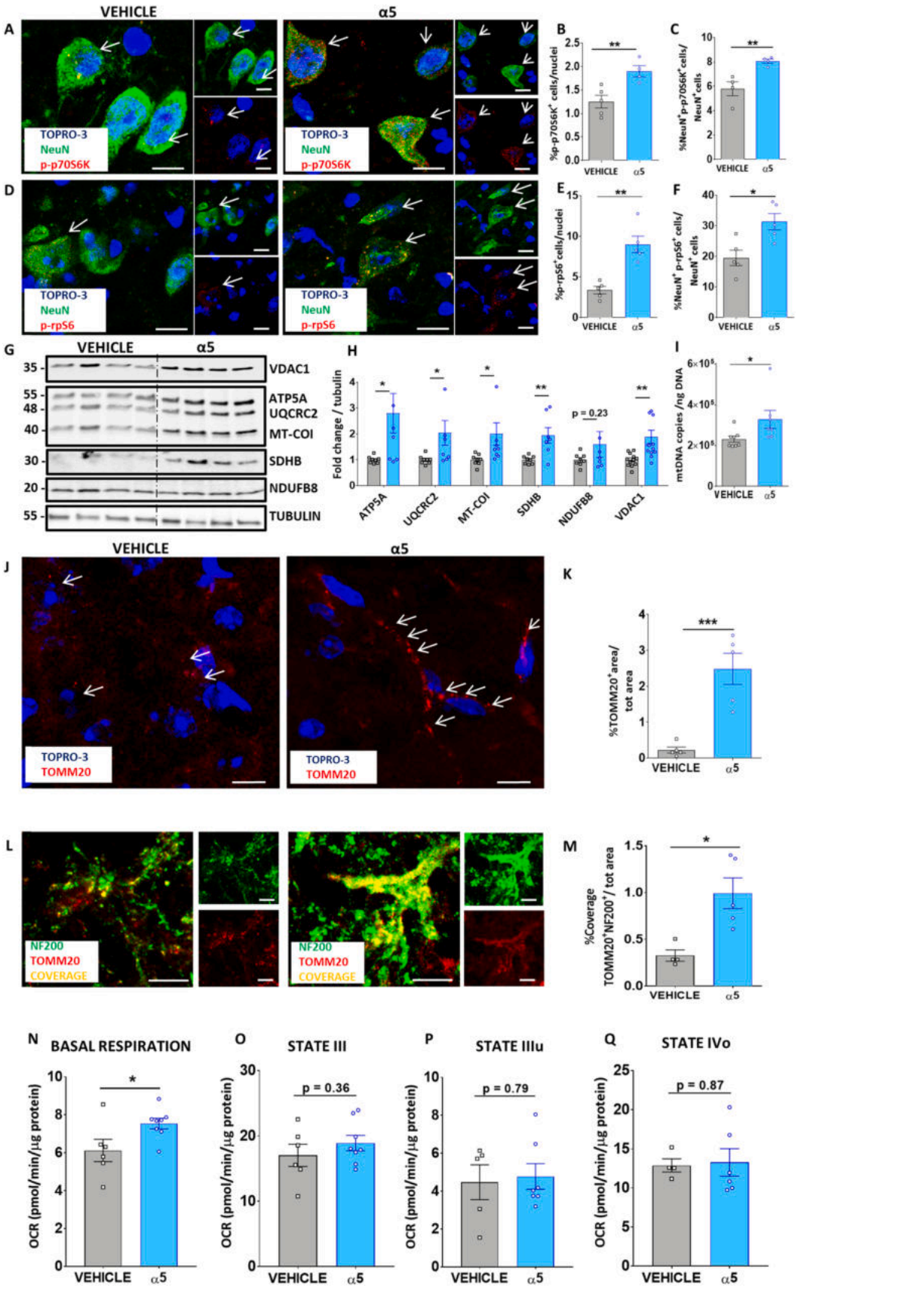

(caption on next page)

Fig. 2. α5 supplementation activated the mTORC1 pathway and improved mitochondrial function in SCI. A) Immunostaining of p-p70S6K$^+$ cells (white arrows) in the perilesional spinal cord sections and quantitative analysis performed on B) total nuclei and C) total NeuN$^+$ cells. D) Immunostaining of p-rpS6$^+$ cells (white arrows) in the perilesional spinal cord sections and quantitative analysis performed on E) total nuclei and F) total NeuN$^+$ cells. N = 5 mice/group for A-F. G) Representative immunoblot of OXPHOS subunits and of the mitochondrial marker VDAC1 of vehicle- and α5-treated lesioned spinal cord sections (see Fig. 1 A). H) Quantitative analysis of the immunoblot normalized to the signal of tubulin and expressed as fold-change compared to the vehicle-treated mice (n = 9 mice/group). I) mtDNA molecules/ng of DNA extracted from the lesioned spinal cord sections (n = 7–8 mice/group). J) Immunostaining of TOMM20$^+$ spots (white arrows) in longitudinal sections of the perilesional spinal cord and K) quantitative analysis. L) TOMM20$^+$/NF200$^+$ coverage and M) quantitative analysis. N = 5 mice/group for J-M. N) Basal respiration of mitochondria extracted from the lesioned spinal cord tissues; other parameters include O) ADP-driven respiration (state III), P) uncoupled respiration (state IIIu) and Q) ATP-linked respiration (state IVo). The mitochondrial respiration (N-Q) was analyzed on n = 6 vehicle- and n = 8 α5-treated mice. The quantifications of TOMM20, Neurofilament-200 and of the coverage of TOMM200/Neurofilament-200 were expressed as percentage of positive area/total area considered. Data in A-F and J-M refer to the perilesional area of the spinal cord analyzed at 34 DPI. Data in G-I and N-Q refer to the site of the lesion at 14 DPI. Data are expressed as mean ± SEM, statistical analysis was performed with unpaired t-test, * $p < 0.05$, * * $p < 0.01$, * ** $p < 0.005$ and * ** * $p < 0.001$. Pictures A, D, J, L are maximum intensity projections of z-stack confocal images. Scale bars: 10 μm in A, D, J and 5 μm in L.

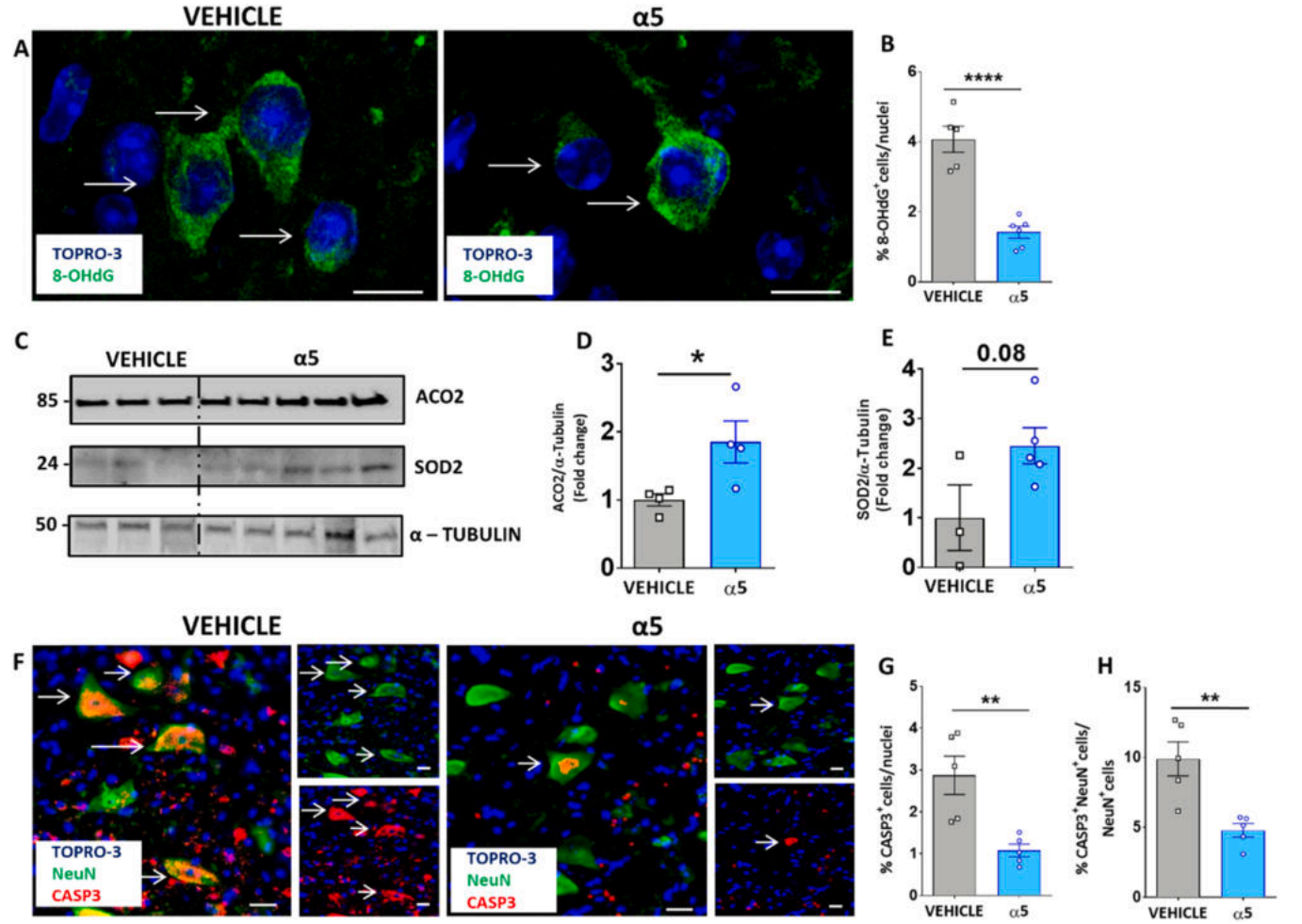

Fig. 3. α5 supplementation decreased the oxidative damage and apoptotic marker in SCI at 34 DPI. A) Oxidative damage detected as 8-OHdG$^+$ staining (white arrows) in the perilesional spinal cord sections and B) quantitative analysis. C) Representative immunoblot of ACO2 and SOD2 performed in vehicle- and α5-treated lesioned spinal cord sections (see Fig. 1 A), and D) and E) quantitative analysis referred to n = 4–5 mice/group. F) Immunostaining of cleaved Caspase-3$^+$ cells in the perilesional spinal cord sections and quantitative analysis referred on G) total nuclei and H) total NeuN$^+$ cells; white arrows represent double-positive cells. N = 5–6 mice/group. Data are expressed as mean ± SEM, statistical analysis was performed by unpaired t-test, * * $p < 0.01$ and * ** * $p < 0.001$. Pictures A and C are maximum intensity projections of z-stack confocal images. Scale bars: 10 μm in A and C.

cysteine, with a pyridoxal phosphate requiring step [36]; such substrates and cofactors are part of the α5 formulation (Table 1) [15]. Thiamine metabolism was impaired in the vehicle-treated SCI mice, and it was significantly, albeit partially, rescued in the α5-treated group (Fig. 1F, G). Glutathione pathway and oxPPP were strongly increased in the spinal cords of α5-treated mice (Fig. 1G), suggesting augmented antioxidant defense. Furthermore, following α5 treatment, we observed an increase of arginine biosynthesis in the spinal cords of α5-treated mice (Fig. 1F, G). Arginine is a key amino metabolite that drives macrophage polarization [37,38].

These data demonstrated that oral administration of the α5 modulated the injured spinal cord metabolism supporting the restoration of TCA cycle intermediates, and metabolic pathways involved in mitochondrial OXPHOS, neuroprotection, and inflammatory response.

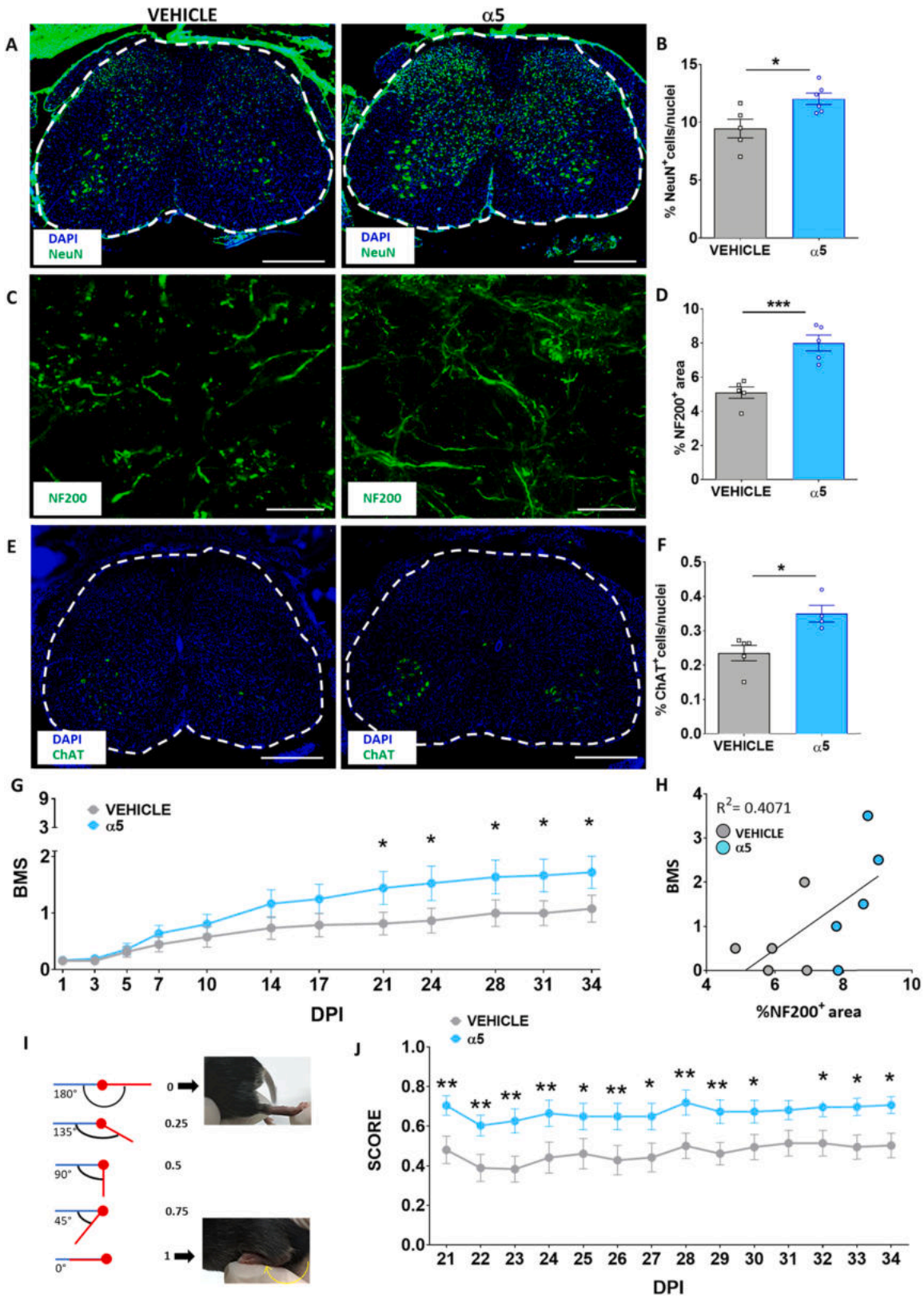

Fig. 4. Functional metabolic rewiring promoted neuronal survival and a partial motor recovery after SCI. A) Immunostaining of NeuN^{+} cells in transversal sections of the perilesional spinal cord and B) quantitative analysis. C) Immunostaining of NF200^{+} cells and D) quantitative analysis. E) Cholinergic neurons detected by ChAT^{+} immunostaining and F) quantitative analysis. N = 5–6 mice/group in A-F. G) BMS locomotor score of vehicle- and α5-treated mice, n = 24–25 mice/group. H) Linear regression between BMS and neurofilament amounts represented as NF200^{+} area. I) Schematic score representation of the evaluation of ankle flexibility. J) Ankle flexibility score of vehicle- and α5-treated mice (n = 21 and 15 mice/group, respectively). Data are expressed as mean ± SEM, statistical analysis was performed with unpaired t-test (B, D, F) and 2-way ANOVA with repeated measurements (G and J) * $p < 0.05$, * ** $p < 0.005$. Picture C is maximum intensity projections of z-stack confocal images. Scale bars: 500 μm in A and E, 5 μm in C.

Table 1
Composition of α5 mixture andtherapeutic dosage used *in vivo*.

Composition of α5 mixture	% (g/100 g)	Therapeutic administration (mcg/g/day)
L-Leucine	31.09	932.7
L-Lysine chlorhydrate	16.90	507
L-Isoleucine	10.36	310.8
L-Valine	10.36	310.8
L-Threonine	7.25	217.5
L-Cysteine	3.11	93.3
L-Histidine	3.11	93.3
L-Phenylalanine	2.07	62.1
L-Methionine	1.04	31.2
L-Tyrosine	0.62	18.6
L-Tryptophan	2.07	62.1
Vitamin B1 (Thiamine chlorhydrate)	0.004	0.12
Vitamin B6 (Pyridoxine chlorhydrate)	0.0038	0.114
Citric acid anhydrous	8.00	240
Malic acid	2.00	60
Succinic acid	2.00	60

3.2. α5 supplementation activates the mTORC1 pathway and increases mitochondrial OXPHOS metabolism in damaged spinal cord tissue after severe SCI

To assess whether the changes in the injured spinal cord metabolism could increase neural cell anabolism and mitochondrial OXPHOS, we analyzed specific hallmarks of the mTORC1 pathway, *i.e.*, the phosphorylation of the p70S6Kinase (p70S6K) at Thr389 (p-p70S6K), and of the 40 S ribosomal protein S6 (rpS6) at Ser235 and 236 residues (p-rpS6) [39]. We found an upregulation of the p-p70S6K in the spinal cord cells (vehicle-treated group: 1.25 ± 0.13% *vs* α5-treated group: 1.90 ± 0.12%, $p < 0.01$) and in $NeuN^+$ neurons of the α5-treated SCI mice (vehicle-treated group: 5.80 ± 0.57% *vs* α5-treated group: 8.10 ± 0.18%, $p < 0.01$) (Fig. 2A-C). Similarly, the levels of p-rpS6 were significantly elevated in the spinal cord sections of α5-treated *versus* vehicle-treated animals (total cells: vehicle-treated group: 3.39 ± 0.45% *vs* α5-treated group: 9.00 ± 1.02%, $p < 0.01$, $n = 4–5$ mice/group; $NeuN^+$ cells: vehicle-treated group: 19.55 ± 2.51% *vs* α5-treated group: 31.35 ± 2.64%, $p < 0.01$, Fig. 2D-F).

Accordingly, the mitochondrial respiratory chain complex subunits NDUFB8 (complex I), SDHB (complex II), UQCRC2 (complex III), MT-COI (complex IV), alpha subunit ATP5A (complex V), and the mitochondrial outer membrane marker VDAC1 [40] were upregulated in the α5-treated compared to vehicle-treated injured spinal cords (Fig. 2 G, H). Consistently, the number of mtDNA molecules extracted from the injured spinal cord was higher in the α5-treated compared to vehicle-treated mice (vehicle-treated group: $2.45 \times 10^5 \pm 0.16 \times 10^5$ *vs* α5-treated group: $3.18 \times 10^5 \pm 0.32 \times 10^5$ mtDNA molecules/ng of DNA, $p < 0.05$, Fig. 2I), and the mitochondrial outer membrane marker TOMM20 was significantly higher in the longitudinal section of the spinal cord tissue of α5-treated compared to vehicle-treated mice (vehicle-treated group: 0.22 ± 0.08% *vs* α5-treated group: 2.48 ± 0.43%, $p < 0.001$, Fig. 2 J, K), confirming the increased mitochondrial mass. Since mitochondria are required for axonal regeneration [16], we also quantified the content of axonal mitochondria. The percentage of coverage between TOMM20 and the neurofilament marker NF200 signals was increased in the α5-treated compared to vehicle-treated mice (vehicle-treated group: 0.33 ± 0.06% *vs* α5-treated group: 0.99 ± 0.16%, $p < 0.01$, Fig. 2 L, M). The markers of mitochondrial dynamics were, however, not affected by the administration of the α5 (Suppl. Fig. S2A-D), suggesting that, in pathological conditions, oxidative substrates, TCA cycle intermediates, and cofactors preferentially support mitochondrial survival and function rather than modulate the mitochondrial network [13]. In line with this observation, the basal respiration of mitochondria obtained from the lesioned spinal cord in the presence of mitochondrial complex I (glutamate and malate) and complex II (succinate) substrates was higher in the α5-treated group (oxygen consumption rate of vehicle-treated mitochondria: 6.12 ± 0.59 pmol/min/μg protein *vs* α5-treated mitochondria: 7.54 ± 0.27 pmol/min/μg protein $p < 0.05$, $n = 6–8$ mice/group, Fig. 2 N), suggesting a more efficient OXPHOS capacity at the basal state. No significant differences were found in state III, state IIIu and state IVo of mitochondrial respiration (Fig. 2O-Q).

Consistent with the increase of glutathione metabolism and oxPPP (Fig. 1H), we found that the reactive oxygen species (ROS) content at the site of the lesion, evaluated by 8-OHdG staining, was considerably attenuated in the α5-treated group (vehicle-treated group: 4.07 ± 0.37% *vs* α5-treated group: 1.42 ± 0.17%, $p < 0.0005$, $n = 5–6$ mice/group, Fig. 3 A, B); accordingly the protein levels of Aconitase 2 (ACO2, vehicle-treated group: 1.00 ± 0.09 *vs* α5-treated group: 1.85 ± 0.31, $p < 0.037$, $n = 4$ mice/group, Fig. 3 C, D) were also increased in the α5-treated mice, suggesting a preserved mitochondrial function and reduced ROS damage. Moreover, the protein levels of the mitochondrial detoxifying enzyme Superoxide dismutase 2 (SOD2) were increased in the spinal cord tissues of α5-treated mice, suggesting an increased oxidative defense (vehicle-treated group: 1.00 ± 0.66 *vs* α5-treated group: 2.45 ± 0.36, $p < 0.08$, n = mice/group n = 3–5 mice/group Fig. 3 C, E). Accordingly, apoptotic cells, which were detected by the cleaved form of caspase-3, were significantly reduced in α5-treated spinal cord sections of the perilesional area (0.4 cm above and below the site of the lesion; vehicle-treated group: 2.87 ± 0.45% *vs* α5-treated group:1.07 ± 0.15, $p < 0.005$, Fig. 3 F, G). Similarly, neuronal cell apoptosis was significantly reduced in the α5-treated mice (vehicle-treated group: 9.90 ± 1.22% *vs* α5-treated group: 4.80 ± 0.49%, $p < 0.005$, Fig. 3 H).

Taken together, these results indicated that the administration of mitochondrial substrates and cofactors activated the mTORC1 anabolic pathway, the OXPHOS metabolism, and ROS defense system in the injured spinal cords, effectively preventing neural cell death.

3.3. α5 supplementation mitigates the damage of the spinal cord tissue and promoted partial motor recovery after severe SCI

SCI disconnects the axons of the corticospinal and the reticulospinal tracts from their postsynaptic targets, disrupting the original circuit. The neural tissue loss also generates an intense local inflammation which determines progressive cyst surrounded by glial/fibrotic scar protecting the neural network from further damage [41], but also inhibiting the axonal elongation and regeneration [42,43].

The degeneration of the spinal cord resulting from the initial mechanical injury is followed by a secondary insult that determines further destruction of neuronal cells, demyelination, neuronal and axonal loss [44]. Therefore, we evaluated the neuroprotective effect of the α5 treatment in severe SCI. Both the size of the scar-encased cyst (Suppl. Fig. S3A, B) and the severity of demyelination (Suppl. Fig. S3C, D) were similar between the vehicle- and α5-treated groups.

The improvement of metabolic and mitochondrial function and the reduction of oxidative damage and cell apoptosis suggested a neuroprotective potential of the α5 treatment. Accordingly, more $NeuN^+$ cells (Fig. 4 A) were present in the perilesional spinal cord parenchyma of the α5-treated compared to vehicle-treated mice (vehicle-treated group: 9.46 ± 0.80%*vs* α5-treated group: 12.03 ± 0.49% $p < 0.05$, Fig. 4B). Similarly, the neurofilament content (NF200), whose expression is closely related to the axonal outgrowth and neuronal homeostasis [45] was higher in the longitudinal sections of α5-treated spinal cord than in those of vehicle-treated mice (vehicle-treated group: 5.10 ± 0.33%, *vs* α5-treated group: 8.00 ± 0.46% $p < 0.001$, Fig. 4 C, D). Notably, spinal motor neurons detected by Choline acetyltransferase (ChAT) enzyme-immunostaining were more abundant in the ventral horns of α5-treated compared to vehicle-treated mice (vehicle-treated group: 0.23 ± 0.02% *vs* α5-treated group 0.35 ± 0.03% $p < 0.05$, Fig. 4E, F).

Altogether, these results indicated that the metabolic modulation of the spinal cord favored motor neuronal survival and corticospinal tract improvement.

To evaluate their impacts on motor recovery, we assessed the BMS score of α5- and vehicle-treated mice (Fig. 4 G). After SCI, mice underwent grave disability as indicated by a BMS $\leq$ 0.5 (Fig. 4 G). The α5-treated group exhibited a mild, yet progressive, improvement of the locomotor performance compared to vehicle-treated mice, reaching a significant and stable partial recovery from 21 DPI (vehicle-treated group: 0.81 *vs* α5-treated group: 1.44, $p < 0.05$, n = 18–19 mice/group Fig. 4 G) corresponding to the movement of the ankle [18]. Interestingly, the progress correlated with the abundance of neurofilaments in the longitudinal sections of the perilesional injured spinal cord (Fig. 4H). Spasticity - a symptom of the upper motor neuron impairment - is a common hallmark resulting from an injury, and it is a major cause of disability in individuals affected by a variety of CNS diseases and trauma. In our model, the severe injury of the spinal cord was associated with the onset of intrinsic tonic spasticity - evaluated through the analysis of the assisted movement of the ankle joint (Fig. 4I and *Materials and Methods, Section 2.4*) from 21 DPI onwards - which was less severe in the α5-treated SCI mice (Fig. 4 J). Collectively, these data showed a significant increase in neuronal cell number and partial improvement of the motor functions of the α5-treated mice.

3.4. α5 administration promotes the activation of microglia in the perilesional spinal cord

Following α5 treatment, we observed an increase of arginine biosynthesis in the spinal cords of treated mice. Arginine is a key amino metabolite that drives macrophage polarization into the pro-regenerative M2 phenotype [37,38]. Therefore, we compared the microglia/macrophages content in the injured spinal cord and we found an increased number of cells expressing the microglia/macrophages marker IBA1 in the α5-treated compared to vehicle-treated mice (vehicle-treated group: 6.00 ± 0.70% *vs* α5-treated group: 9.22 ± 0.81% $p < 0.05$, n = 5 mice/group, Fig. 5 A, B). Since the morphology and functions of the immune-inflammatory cells are tightly coupled, we quantified the proportion of $IBA1^+$ cells with either ramified (resting), or amoeboid (activated) phenotypes [46]. The activated round-ameboid $IBA1^+$ cells were significantly increased in the spinal cord parenchyma of α5-treated mice (vehicle-treated group: 21.59 ± 1.61% *vs* α5-treated group: 37.29 ± 1.60%, $p < 0.01$, Fig. 5 C, D). Moreover, the percentage of cells expressing the M2 marker CD206 [47] was higher in the spinal cord parenchyma of α5-treated mice (vehicle-treated group: 5.07 ± 2.26%, *vs* α5-treated group: 9.11 ± 0.81% *vs* $p < 0.01$, Fig. 5E, F).

To specifically assess the microglial response, we double-stained the spinal cord sections with the microglia-specific marker TMEM119 and with the IBA1 marker [48]. We observed that TMEM119/IBA1 double-positive cells increased in α5-treated injured spinal cord (vehicle-treated group: 1.19 ± 0.20% *vs* α5-treated group: 3.31 ± 0.78%, $p < 0.03$, n = 5 mice/group, Fig. 5 G, H). Moreover, the $CD206^+/TMEM119^+$ cells also increased in α5-treated mice, suggesting an increase of M2 phenotype (vehicle-treated group: 0.98 ± 0.16% *vs* α5-treated group: 2.83 ± 0.78%, $p < 0.048$, n = 5 mice/group, Fig. 5I, J). However, despite acute (72 h) treatment of microglial cells with α5 was able to upregulate genes involved in acute inflammation (*Cox-2, Il-1β, Il-6*, Suppl. Fig. S4A) and in microglial phenotypes, (*iNos, Arg1* and *Socs-3*, Suppl. Fig. S4A), we observed only minor modification of the expression of microglia markers (Suppl. Fig. S4B), and we failed to detect any modification in mitochondrial mass (Suppl. Fig. S4C, E), OXPHOS metabolism (Suppl. Fig. S4F, G), or the activation of the mTORC1 pathway (Suppl. Fig. S4C, D). These results suggested that α5 administration triggered only a partial metabolic modification of microglial cells *in vitro*.

Altogether, these data indicated that α5 treatment increased the fraction of microglial cells with an activated ameboid phenotype and expressing the CD206 marker, suggestive of pro-regenerative M2 traits in the spinal cord parenchyma.

4. Discussion

In this study, we evaluated the therapeutic effects of increased oxidative metabolism in neural tissue after severe contusive SCI. To this aim, we chose a SCI model with complete paralysis of the hindlimbs, and without spontaneous functional recovery, which we obtained by performing a lesion at the level of the T11 vertebra. This model is clinically relevant as it recapitulates one of the most frequent human conditions that results after complete SCI [49] which is still incurable and severely impacts the quality of life of affected patients. Following injury, the neural tissue experiences a dramatic metabolic impairment [5], which involves a decrease of energy metabolism [7,8], and a severe reduction of precursor availability, including aspartate, glutamate [5], and BCAAs [50,51].

We aimed to restore the oxidative metabolism in a mouse model of severe contusive SCI by a chronic oral administration of the α5 metabolic substrates. We previously tested various compositions *in vitro* on differentiating neural stem cells [15]. We achieved the best results on the modulation of mitochondrial metabolism with α5 that, contrary to the other mixtures, also contains Kreb's cycle intermediates malate, citrate, and succinate (Table 1) [15]. Hence, we assessed the α5 effects on spinal cord metabolism, mitochondrial function, ROS defense system, neural cell survival, immune cell activation, and motor recovery. Our study was designed as a therapeutic intervention. Therefore, the oral administration of α5 started three days after the severe SCI. Although the molecular effects of a BCAA-treatment can be maximized by a circadian administration [52], we opted for a continuous supplementation of α5 in drinking water, as a timely oral gavage may have exposed the injured mice to a high risk of fatal lesions. We analyzed the metabolic state of the spinal cords at 14 DPI and the tissue histology at 34 DPI. Since the locomotor improvement of the α5-treated group was appreciable in the BMS curve at 14 DPI (Fig. 4 G), this time point was selected for metabolomics analysis. We reasoned that tardive metabolic evaluation of the tissue could have led to the detection of chronic, compensatory alteration of the tissue metabolism rather than acute, α5-mediated metabolic changes. By contrast, the time point of 34 DPI was selected to evaluate the chronic histological changes occurring on the lesioned spinal cord upon α5-treatment.

Metabolomic analysis revealed significant impairment of the cellular metabolism following SCI and a substantial decline of the TCA cycle. Interestingly, our data indicated a significant upregulation of the glycolytic pathway in vehicle-treated spinal cords compared to the healthy uninjured group, suggesting the activation of a compensatory mechanism to produce ATP in response to the decrease of the TCA cycle. In the α5-treated samples, TCA cycle intermediates were restored, suggesting a shift towards a more physiological oxidative metabolism. The administered BCAAs and EAAs can feed TCA cycle through anaplerotic reactions leading to the production of succinyl-CoA (through the breakdown of isoleucine, methionine, and valine), and α-ketoglutarate and oxaloacetate by transamination and deamination of any amino acids [53]. Indeed, microscale oxygraphy performed on isolated mitochondria from the lesioned spinal cords revealed increased basal respiration in the α5-treated group, indicating a higher proton current generated by mitochondrial respiratory chain enzymes [54]. In addition, we found in α5-treated mice an increased number of mitochondria and mitochondrial respiratory chain subunits at the site of the lesion (Fig. 2 G-Q), including in neuronal cells (Fig. 2 L, M). Consistently, we observed the activation of the anabolic mTORC1-signaling cascade in the resident spinal cord cells and neurons of the α5-treated mice. The mTORC1 pathway has an essential role in cellular anabolism, morphogenesis, and survival, and it can be activated in the α5-treated injured spinal cord by both the direct action of the amino acids, mostly leucine [28,29], administered in the treatment, and by the increase of the cellular ATP

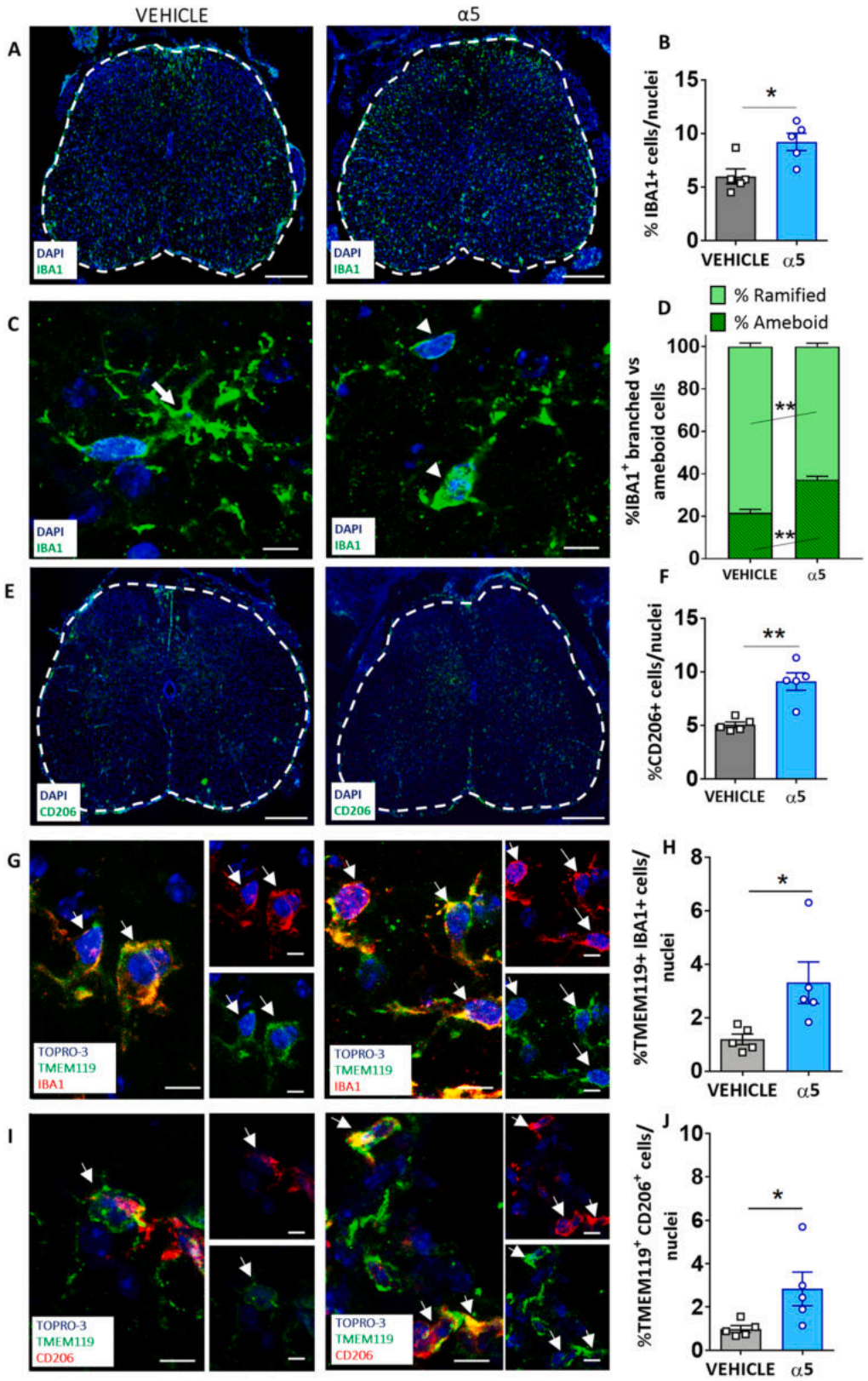

Fig. 5. Functional metabolic rewiring promoted the activation of the microglia in the perilesional spinal cord. A) Immunostaining of IBA1$^+$ cells and B) quantitative analysis. C) Immunostaining of IBA1$^+$ cells with ramified (white arrows) or ameboid (white arrowheads) morphologies. D) Percentage of the IBA1$^+$ cells displaying ameboid or ramified morphologies. E) Immunostaining of CD206$^+$ cells and F) quantitative analysis. G) Immunostaining of TMEM119$^+$/IBA1$^+$ cells (white arrows) and H) quantitative analysis. I) Immunostaining of CD206$^+$/TMEM119$^+$ cells (white arrows) and J) quantitative analysis. N = 5 mice/group in A-J. Data are expressed as mean ± SEM, statistical analysis was performed with unpaired t-test, *$p < 0.05$, * * $p < 0.01$, * ** $p < 0.005$. Pictures C, G and I are maximum intensity projections of z-stack confocal images. Scale bars: 500 μm in A and E, 10 μm in C, G and I.

content resulting from the increase of oxidative metabolism [15,31].

Moreover, the metabolomic analysis indicated an increase of phosphatidylinositols in the α5-treated injured spinal cord (Fig. 1H), which may also positively regulate the activation of mTORC1 [55], further supporting the therapeutic effect of the treatment. These data confirm the well-documented [24,32,56–58] mitochondriogenic effects of BCAA- and EAA-enriched combinations *in vitro* and *in vivo*. However, we didn't observe a mitochondrial network remodeling as we previously reported in differentiating neural stem cells (NSCs) *in vitro* [15]. Different concentrations and duration of the treatment, and the impact of the pathological environment on *in vivo* cell behavior may explain different effects on mitochondrial response.

Our data are in line with previous findings which pointed to a critical mitochondrial dysfunction following SCI [8,9,16,34], and remarkably demonstrate that a functional metabolic rewiring could be exerted in severe contusive SCI by oral administration of therapeutic substrates.

As observed on neuronal cells *in vitro* [15], the α5 treatment boosted the ROS defense system in the lesioned spinal cords. This effect was supported by the increased activation of the oxPPP and glutathione pathway (Fig. 1 F, H). Reduced glutathione (GSH) takes part in the antioxidant defense system and detoxification from mitochondrial ROS. The oxPPP branches from glucose 6-phosphate (G6P) to produce NADPH, acting as a major regulator for cellular redox homeostasis and biosynthesis. Such metabolic changes were accompanied by the reduction of oxidative damage (Fig. 3 A, B) cleaved caspase- 3 (Fig. 3 C, D) and increased cellular survival. Accordingly, α5-treated spinal cords preserved a higher number of neurons, including cholinergic neurons and also neurofilaments that structurally support the axons (Fig. 4 A-F). We found a positive correlation between the amount of NF200 and BMS (Fig. 4H), suggesting that the significant, albeit partial, motor recovery (Fig. 4 G) may reflect the abundance of neuronal cells and axonal circuits in the lesioned spinal cord parenchyma.

The metabolomics analysis also revealed a restoration of thiamine and an increase of taurine concentration in the α5-treated injured spinal cord. Thiamine is a key cofactor for mitochondrial metabolic enzymes, *i.e.* the oxoglutarate dehydrogenase complex (OGDC) and the pyruvate dehydrogenase complex (PDC), which are inactivated in mammalian models of traumatic CNS injury [8,59]; its deficiency causes mitochondrial metabolic impairment, neural tissue damage, and oxidative stress [33]. Taurine is one of the most abundant amino acids in the brain that protects the CNS from further impairment after an injury [36]. In agreement with previous findings [60,61], we observed increased taurine levels in the spinal cords of injured mice, which were further enhanced in the α5-treated SCI group. Data from the literature indicate that acute taurine treatment may enhance axonal regeneration in a lamprey [61] and a murine model of SCI [62]. Altogether, the changes in thiamine and taurine further support the neuroprotective effects of the α5 mixture.

Moreover, an increase of several metabolites involved in immune modulation was observed in the α5-treated spinal cords. Taurine itself may exert neuroprotection through the suppression of microglial M1 polarisation-mediated neuroinflammation [63], while arginine is a key amino metabolite that drives macrophage M2 polarization [37,38]. Accordingly, α5-treated samples displayed a relevant increase of activated microglia population at the site of the lesion, expressing the CD206 marker suggestive of pro-resolutive, M2 phenotype. Interestingly, arginine is synthesized by macrophages from engulfed apoptotic cells through continuous efferocytosis [38], suggesting that a greater clearance of apoptotic cells may occur in the α5-treated lesioned spinal cord [64]. The results of the *in vitro* study showed partial modulation in gene expression, without significant changes in the cellular morphology or metabolism of microglial cells following α5 administration. This could be dependent on i) the dose (α5 at 0.5% w/v in culture medium compared to 3 mg/g/day of the *in vivo* administration); ii) the short incubation time (72 h compared to 31 days *in vivo*); iii) the different developmental stage of the microglia (*in vitro* newborn-derived compared to adult microglia *in vivo* [65]); vi) intrinsic phenotypic differences due to the different tissue of origin of the microglia (brain-derived microglia *in vitro* compared to spinal cord microglia *in vivo* [66]). These factors could account for the divergences observed between the *in vivo* and *in vitro* data. Finally, M2-polarised microglia may prefer different substrates for oxidative metabolism, including glutamine/glutamate and fatty acids [37,67], that could not be unraveled by a standard Mitostress assay. Overall, the results we obtained pointed toward a significant upregulation of immune cells in the spinal cord, whether this was obtained through a direct or indirect effect of the α5 mixture on the immune cell's metabolism may not be concluded. However, it is worth emphasizing such relevant effects on immune cells obtained by oral administration of metabolic precursors.

In conclusion, our findings highlight novel and previously uncharacterized proof-of-concept observations showing that a therapeutic functional metabolic rewiring of the injured spinal cord could effectively reduce neural tissue damage, activate the anabolic mTORC1 pathway, increase the mitochondrial function, the ROS defense, and microglia/macrophages activation, leading to a partial improvement of motor recovery.

CRediT authorship contribution statement

Sissi Dolci: Investigation, Methodology, Software, Formal analysis, Data curation, Visualisation. **Loris Mannino**: Investigation, Formal analysis, Visualisation, Validation. **Emanuela Bottani:** Investigation, Formal analysis, Writing – original draft, Writing – review & editing. **Alessandra Campanelli:** Investigation, Formal analysis, Visualisation Validation. **Marzia Di Chio**: Investigation. **Stefania Zorzin**: Investigation. **Giulia D'Arrigo**: Investigation. **Alessia Amenta**: Investigation; **Agnese Segala**: Investigation. **Giuseppe Paglia**: Investigation, Formal Analysis. **Vanna Denti**: Investigation, Formal analysis. **Guido Fumagalli**: Conceptualization, Supervision. **Enzo Nisoli**: Funding acquisition, Conceptualization, Methodology. **Alessandra Valerio**: Funding acquisition, Conceptualization, Methodology, Formal Analysis. **Claudia Verderio**: Conceptualization, Investigation, Supervision. **Giuseppe Martano**: Conceptualization, Investigation, Formal Analysis. **Francesco Bifari**: Conceptualization, Methodology, Writing – original draft, Writing – review & editing, Supervision, Funding acquisition. **Ilaria Decimo:** Conceptualization, Methodology, Writing – original draft, Supervision, Writing – review & editing, Funding acquisition.

Author contributions

I.D. and F.B. designed the research; S.D., L.M., E.B., A.C., M.D.C., S.Z. performed *in vivo* research; G.D'A., A.A., A.S. performed *in vitro* research; G.P., V.D., G.M. performed metabolomics analysis; S.D., L.M., E.B., A.C analyzed the data; I.D., F.B., G.F., C.V. E.N., A.V discussed and interpreted the data; I.D., F.B., G.F., E.B. wrote the manuscript.

Declaration of Competing Interest

None.

Acknowledgments

We thank the "Centro Piattaforme Tecnologiche "CPT of the University of Verona (IT) for the analysis of mtDNA. This work is supported by Italian patient association la Colonna and GALM; Fondazione Cariverona (Grant number 2017–0604) to I.D. and G.F.; Fondazione Telethon–Italy (Grant Number GSP20004_PAsMCT8006) to I.D and E.B.; Fondazione Telethon–Italy (Grant Number GGP19250) and MS Alliance (Grant Number PA-2001–35858) to F.B.;European Union project FET-PROACT-2018–2020 HERMES.; Cariplo (grant # 2016–1006) to E.N. and A.V; A.A. was supported by Doctoral school in Experimental Medicine, Università degli Studi di Milano, Italy; this project has received

funding from the European Union's Horizon 2020 research and innovation programme under grant agreement HERMES No 824164" to I.D.

Appendix A. Supporting information

Supplementary data associated with this article can be found in the online version at doi:10.1016/j.phrs.2022.106149.

References

[1] D.D. Clarke, S.L, Regulation of cerebral metabolic rate, in: A.B. Siegel GJ, R. W. Albers (Eds.), Basic Neurochemistry: Molecular, Cellular and Medical Aspects, Lippincott-Raven, Philadelphia, 1999.
[2] S.B. Laughlin, R.R. de Ruyter van Steveninck, J.C. Anderson, The metabolic cost of neural information, Nat. Neurosci. 1 (1) (1998) 36–41.
[3] S. Hallermann, et al., State and location dependence of action potential metabolic cost in cortical pyramidal neurons, Nat. Neurosci. 15 (7) (2012) 1007–1014.
[4] A. Hasenstaub, et al., Metabolic cost as a unifying principle governing neuronal biophysics, Proc. Natl. Acad. Sci. USA 107 (27) (2010) 12329–12334.
[5] Y. Fujieda, et al., Metabolite profiles correlate closely with neurobehavioral function in experimental spinal cord injury in rats, PloS One 7 (8) (2012), e43152.
[6] R. LoPachin, et al., Experimental spinal cord injury: spatiotemporal characterization of elemental concentrations and water contents in axons and neuroglia, J. Neurophysiol. 82 (5) (1999) 2143–2153.
[7] Y. Cao, et al., Mitochondrial fusion and fission after spinal sacord injury in rats, Brain Res. 1522 (2013) 59–66.
[8] S. Patel, et al., Acetyl-L-carnitine ameliorates mitochondrial dysfunction following contusion spinal cord injury, J. Neurochem. 114 (1) (2010) 291–301.
[9] P. Sullivan, et al., Temporal characterization of mitochondrial bioenergetics after spinal cord injury, J. Neurotrauma 24 (6) (2007) 991–999.
[10] G. Martano, et al., Metabolism of stem and progenitor cells: proper methods to answer specific questions, Front Mol. Neurosci. 12 (2019) 151.
[11] C. Lange, et al., Relief of hypoxia by angiogenesis promotes neural stem cell differentiation by targeting glycolysis, EMBO J. 35 (9) (2016) 924–941.
[12] A. Quaegebeur, et al., Deletion or inhibition of the oxygen sensor PHD1 protects against ischemic stroke via reprogramming of neuronal metabolism, Cell Metab. 23 (2) (2016) 280–291.
[13] E. Motori, et al., Neuronal metabolic rewiring promotes resilience to neurodegeneration caused by mitochondrial dysfunction, eaba8271 6 (35) (2020).
[14] D. Welin, et al., Effects of N-acetyl-cysteine on the survival and regeneration of sural sensory neurons in adult rats, Brain Res. 1287 (2009) 58–66.
[15] F. Bifari, et al., Complete neural stem cell (NSC) neuronal differentiation requires a branched chain amino acids-induced persistent metabolic shift towards energy metabolism, Pharm. Res. 158 (2020), 104863.
[16] Q. Han, et al., Restoring cellular energetics promotes axonal regeneration and functional recovery after spinal cord injury, Cell Metab. 31 (3) (2020) 623–641.
[17] I. Decimo, et al., Nestin- and doublecortin-positive cells reside in adult spinal cord meninges and participate in injury-induced parenchymal reaction, Stem Cells 29 (12) (2011) 2062–2076.
[18] D. Basso, et al., Basso Mouse Scale for locomotion detects differences in recovery after spinal cord injury in five common mouse strains, J. Neurotrauma 23 (5) (2006) 635–659.
[19] J. Charles, et al., Musculoskeletal geometry, muscle architecture and functional specialisations of the mouse hindlimb, PloS One 11 (4) (2016), e0147669.
[20] G. Martano, et al., Biosynthesis of glycerol phosphate is associated with long-term potentiation in hippocampal neurons, Metabolomics 12 (8) (2016) 1–8.
[21] G. Martano, et al., Biosynthesis of astrocytic trehalose regulates neuronal arborization in hippocampal neurons 8 (9) (2017) 1865–1872.
[22] C. Volani, et al., Pre-analytic evaluation of volumetric absorptive microsampling and integration in a mass spectrometry-based metabolomics workflow, Anal. Bioanal. Chem. 409 (26) (2017) 6263–6276.
[23] S. Dolci, et al., High yield of adult oligodendrocyte lineage cells obtained from meningeal biopsy, Front Pharm. 8 (2017) 703.
[24] D. Brunetti, et al., Targeting multiple mitochondrial processes by a metabolic modulator prevents sarcopenia and cognitive decline in SAMP8 Mice, Front Pharm. 11 (2020) 1171.
[25] P. Quiros, et al., Analysis of mtDNA/nDNA ratio in mice, Curr. Protoc. mouse Biol. 7 (1) (2017) 47–54.
[26] G. Faustini, et al., Alpha-synuclein preserves mitochondrial fusion and function in neuronal cells, Oxid. Med. Cell. Longev. (2019) 4246350.
[27] C. Ruocco, et al., Essential amino acid formulations to prevent mitochondrial dysfunction and oxidative stress, Curr. Opin. Clin. Nutr. Metab. care 24 (1) (2021) 88–95.
[28] C. Lynch, et al., Regulation of amino acid-sensitive TOR signaling by leucine analogues in adipocytes, J. Cell. Biochem. 77 (2) (2000) 234–251.
[29] H. Fox, et al., Amino acid effects on translational repressor 4E-BP1 are mediated primarily by L-leucine in isolated adipocytes, Am. J. Physiol. 275 (5) (1998) c1232–c1238.
[30] C. Ruocco, et al., Manipulation of dietary amino acids prevents and reverses obesity in mice through multiple mechanisms that modulate energy homeostasis, Diabetes 69 (11) (2020) 2324–2339.
[31] S. Schieke, et al., The mammalian target of rapamycin (mTOR) pathway regulates mitochondrial oxygen consumption and oxidative capacity, J. Biol. Chem. 281 (37) (2006) 27643–27652.
[32] L. Tedesco, et al., A special amino-acid formula tailored to boosting cell respiration prevents mitochondrial dysfunction and oxidative stress caused by doxorubicin in mouse cardiomyocytes, Nutrients 12 (2) (2020) 282.
[33] G. Gibson, et al., Vitamin B1 (thiamine) and dementia, Ann. N. Y. Acad. Sci. 1367 (1) (2016) 21–30.
[34] M. McEwen, et al., Targeting mitochondrial function for the treatment of acute spinal cord injury. Neurotherapeutics: the journal of the American Society for Experimental, NeuroTherapeutics 8 (2) (2011) 168–179.
[35] A. Marat, V. Haucke, Phosphatidylinositol 3-phosphates-at the interface between cell signalling and membrane traffic, EMBO J. 35 (6) (2016) 561–579.
[36] R. Gupta, Y. Seki, J. Yosida, Role of taurine in spinal cord injury, Curr. Neurovascular Res. 3 (3) (2006) 225–235.
[37] M. Kieler, M. Hofmann, G. Schabbauer, More than just protein building blocks: how amino acids and related metabolic pathways fuel macrophage polarization. The, FEBS J. 288 (12) (2021) 3694–3714.
[38] A. Yurdagul, et al., Macrophage metabolism of apoptotic cell-derived arginine promotes continual efferocytosis and resolution of injury, Cell Metab. 31 (3) (2020) 518–533.
[39] R. Pearson, et al., The principal target of rapamycin-induced p70s6k inactivation is a novel phosphorylation site within a conserved hydrophobic domain, EMBO J. 14 (21) (1995) 5279–5287.
[40] E. Bugiardini, et al., Expanding the molecular and phenotypic spectrum of truncating MT-ATP6 mutations, Neurol. Genet 6 (1) (2020), e381.
[41] J. Faulkner, et al., Reactive astrocytes protect tissue and preserve function after spinal cord injury, J. Neurosci.: Off. J. Soc. Neurosci. 24 (9) (2004) 2143–2155.
[42] G. Rooney, et al., Importance of the vasculature in cyst formation after spinal cord injury, J. Neurosurg. Spine 11 (4) (2009) 432–437.
[43] M. Fehlings, G. Hawryluk, Scarring after spinal cord injury, J. Neurosurg. Spine 13 (2) (2010) 165–167.
[44] A. Alizadeh, S. Dyck, S. Karimi-Abdolrezaee, Traumatic spinal cord injury: an overview of pathophysiology, models and acute injury mechanisms, Front. Neurol. 10 (2019) 282.
[45] H. Wang, et al., Neurofilament proteins in axonal regeneration and neurodegenerative diseases, Neural Regen. Res. 7 (8) (2012) 620–626.
[46] B. Davis, et al., Characterizing microglia activation: a spatial statistics approach to maximize information extraction, Sci. Rep. 7 (1) (2017) 1576.
[47] F. Martinez, et al., Transcriptional profiling of the human monocyte-to-macrophage differentiation and polarization: new molecules and patterns of gene expression, J. Immunol. (Baltim., Md.: 1950) 177 (10) (2006) 7303–7311.
[48] M. Fumagalli, et al., How to reprogram microglia toward beneficial functions, Glia 66 (12) (2018) 2531–2549.
[49] R. Rupp, Spinal cord lesions, Handb. Clin. Neurol. 168 (2020) 51–65.
[50] R. Paterno, H. Metheny, A. Cohen, Memory deficit in an object location task after mild traumatic brain injury is associated with impaired early object exploration and both are restored by branched chain amino acid dietary therapy, J. Neurotrauma 35 (17) (2018) 2117–2124.
[51] J. Cole, et al., Dietary branched chain amino acids ameliorate injury-induced cognitive impairment, Proc. Natl. Acad. Sci. USA 107 (1) (2010) 366–371.
[52] M.N. Latimer, et al., Branched chain amino acids selectively promote cardiac growth at the end of the awake period, J. Mol. Cell Cardiol. 157 (2021) 31–44.
[53] F. Bifari, E. Nisoli, Branched-chain amino acids differently modulate catabolic and anabolic states in mammals: a pharmacological point of view, Br. J. Pharmacol. 174 (11) (2017) 1366–1377.
[54] M. Brand, D. Nicholls, Assessing mitochondrial dysfunction in cells, Biochem. J. 435 (2) (2011) 297–312.
[55] D. Bridges, et al., Phosphatidylinositol 3,5-bisphosphate plays a role in the activation and subcellular localization of mechanistic target of rapamycin 1, Mol. Biol. Cell 23 (15) (2012) 2955–2962.
[56] G. D'Antona, et al., Branched-chain amino acid supplementation promotes survival and supports cardiac and skeletal muscle mitochondrial biogenesis in middle-aged mice, Cell Metab. 12 (4) (2010) 362–372.
[57] L. Zhang, J. Han, Branched-chain amino acid transaminase 1 (BCAT1) promotes the growth of breast cancer cells through improving mTOR-mediated mitochondrial biogenesis and function, Biochem Biophys. Res Commun. 486 (2) (2017) 224–231.
[58] Y. Tanada, et al., Branched-chain amino acids ameliorate heart failure with cardiac cachexia in rats, Life Sci. 137 (2015) 20–27.
[59] G. Mkrtchyan, et al., Thiamine preserves mitochondrial function in a rat model of traumatic brain injury, preventing inactivation of the 2-oxoglutarate dehydrogenase complex, Biochim. Et. Biophys. Acta Bioenerg. 1859 (9) (2018) 925–931.
[60] D. McAdoo, et al., Changes in amino acid concentrations over time and space around an impact injury and their diffusion through the rat spinal cord, Exp. Neurol. 159 (2) (1999) 538–544.
[61] D. Sobrido-Cameán, et al., Taurine promotes axonal regeneration after a complete spinal cord injury in lampreys, J. Neurotrauma 37 (6) (2020) 899–903.
[62] Y. Nakajima, et al., Taurine reduces inflammatory responses after spinal cord injury, J. Neurotrauma 27 (2) (2010) 403–410.
[63] Y. Che, et al., Taurine protects dopaminergic neurons in a mouse Parkinson's disease model through inhibition of microglial M1 polarization, Cell death Dis. 9 (4) (2018) 435.

[64] V. Bellver-Landete, et al., Microglia are an essential component of the neuroprotective scar that forms after spinal cord injury, Nat. Commun. 10 (1) (2019) 518.
[65] C.A. Brannan, M.R. Roberts, Resident microglia from adult mice are refractory to nitric oxide-inducing stimuli due to impaired NOS2 gene expression, Glia 48 (2) (2004) 120–131.
[66] P.K. Yip, et al., Rapid isolation and culture of primary microglia from adult mouse spinal cord, J. Neurosci. Methods 183 (2) (2009) 223–237.
[67] I. Geric, et al., Metabolic reprogramming during microglia activation, Immunometabolism 1 (2019), e190002.